

Kinetic Simulation of the Enzymatic Oxidation of Methane

E. I. Karasevich, Yu. K. Karasevich, and A. E. Shilov

Emanuel Institute of Biochemical Physics, Russian Academy of Sciences, Moscow, 119334 Russia

e-mail: elka@sky.chph.ras.ru

Received October 24, 2006

Abstract—The kinetics of methane oxidation by methane monooxygenase is simulated numerically. Literature data on the distribution of products of the oxidation of deuterated methane CH_4-nD_n (CH_3D , CH_2D_2 , and CHD_3), as well as on the kinetic isotope effect in the competitive oxidation of CH_4 and CD_4 by methane monooxygenase, are analyzed in the framework of a nonradical multistep mechanism. Kinetic schemes whose first step involves two hydrogen atoms of the oxidation substrate are considered. The kinetic models suggested for methane oxidation are in good agreement with experimental data.

DOI: 10.1134/S0023158408020055

INTRODUCTION

The mechanism of the oxidation of methane, the least reactive saturated hydrocarbon, by the enzymatic systems of methanotrophic bacteria has attracted much attention in recent years [1–3]. The bacterial enzyme methane monooxygenase (MMO) catalyzes methane oxidation by dioxygen according to the following equation:



Although the soluble form of MMO can be obtained from many sources, the enzymes from *Methylosinus trichosporum* OB3b [4] and *Methylococcus capsulatus* (Bath) [5] have been studied in greatest detail. Either enzyme consists of three protein components: hydroxylase (MMOH), reductase, and a regulatory subunit termed the B-component. The methane hydroxylation reaction occurs in the catalytic cycle of MMOH, whose

active site contains a dinuclear iron complex. The MMOH catalytic cycle (Fig. 1) begins with a reduction step in which the initial MMOH species, H_{ox} , is converted into its reduced form, H_{red} . The interaction of the reduced hydroxylase component with oxygen leads, in several steps, to the formation of an intermediate denoted H_{peroxo} , which then rearranges into the intermediate Q. Based on Mössbauer spectroscopy data, this latter intermediate is thought to have a diferryl or bis- μ -oxo complex structure.

The intermediate Q reacts with the substrate to produce an alcohol. It was found that the kinetic isotope effect (KIE) of this process, calculated as the ratio of the rate constants of Q consumption in the bimolecular reactions with CH_4 and CD_4 , has an unusually high value ($k_{\text{H}}/k_{\text{D}} = 50–100$) [6]. The MMO enzyme system can oxidize not only methane, but other hydrocarbons as well [7]. Partial racemization of the reaction prod-

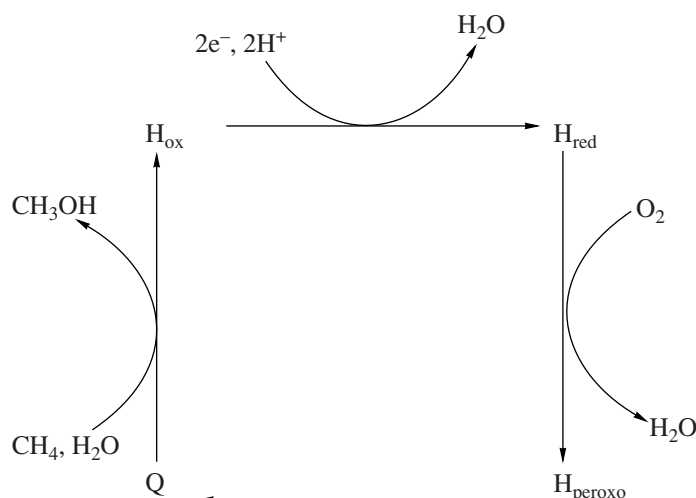


Fig. 1. Catalytic cycle of the MMO hydroxylase component.

ucts was observed in the course of the MMO-catalyzed oxidation of chiral ethane $H(3)H(2)H(1)CCH_3$ [8]. Based on these experimental facts, many researchers [1, 9] currently hold to the hidden-radical mechanism known as the oxygen rebound mechanism (ORM) of the interaction between the intermediate Q and the substrate [10]. However, careful examination of experimental data showed that this hidden-radical mechanism does not withstand quantitative verification [11, 12]. A new, nonradical mechanism was suggested [13], whose essential feature is the formation of an intermediate complex between the substrate and the active site.

Experimental data on the oxidation of deuterated methane (CH_3D , CH_2D_2 , CHD_3) by the MMO enzyme system from *Methylosinus trichosporum* [17] were analyzed in the framework of a nonradical mechanism involving pentacoordinated carbon [14–16]. According to the results of these experiments [17], the KIE value calculated from the reaction product ratios taking into account the number of C–D and C–H bonds in the methane molecule increases significantly with an increasing number of deuterium atoms. The analysis carried out in [16] showed that quantitative agreement between experimental and calculated product distribution data for the MMO-catalyzed hydroxylation of deuterated methane (CH_3D , CH_2D_2 , CHD_3) can be achieved using parameters with simple physical meanings and realistic values only if the reaction yielding the intermediate complex containing pentacoordinated carbon is reversible. Furthermore, it was shown that the decomposition rate of this intermediate complex should be much higher than its formation rate ($w_{-1} \gg w_1$). However, it was found that these conditions lead to incompatibility between the kinetic parameter sets ensuring simultaneous quantitative agreement of the calculated data with experimental product distribution data for partially deuterated methane oxidation and with experimental KIE values for the competitive oxidation of CH_4 and CD_4 by the MMO enzyme system. To resolve this contradiction, the kinetic model of the mechanism under consideration should be further complicated. The purpose of this study is to carry out numerical simulation of the kinetics of methane oxidation by the MMO enzyme system.

COMPUTATIONAL METHOD

Numerical calculations were carried out according to an earlier developed technique [15]. Calculations for methane oxidation kinetic schemes were carried out for various model parameter ratios using a standard direct kinetic problem solver adapted to our system. Since only the ratios of oxidation products were known, the ratios rather than the absolute values of the model parameters were significant for their mathematical description. Numerical solutions that agreed (within the experimental error) with the experimental results for the oxidation of isotope-substituted methane by the MMO system were selected from the total solution set

obtained with different kinetic parameters. The set of kinetic parameters corresponding to steady-state oxidation kinetics was selected for each mechanistic model. In all cases, correspondence to the steady-state kinetic regime was confirmed by the reaction product ratios being the same throughout the oxidation substrate conversion range of 0.1 to 99.9%.

RESULTS AND DISCUSSION

Investigations of kinetic isotope effects in deuterated methane hydroxylation provide important information about the dynamics of the enzymatic oxidation of methane. The simplest and most common method used in this area is the study of the influence of isotope substitutions in the substrate molecule on the rate of Q consumption during hydroxylation by the MMO system.

The oxidation of deuterated methane $CH_{4-n}D_n$ (CH_3D , CH_2D_2 , CHD_3) by soluble MMO from *Methylosinus trichosporum* [17] yields $CH_{3-n}D_nOH$ and $CH_{4-n}D_{n-1}OH$ alcohols in the following ratios:

for CH_3D

$$\rho_1 = [CH_2DOH]/[CH_3OH] = 11.7 \pm 3.0,$$

for CH_2D_2

$$\rho_2 = [CHD_2OH]/[CH_2DOH] = 9.30 \pm 0.54, \quad (1)$$

for CHD_3

$$\rho_3 = [CD_3OH]/[CHD_2OH] = 4.00 \pm 0.33.$$

The $CH_{4-n}D_{n-1}OH$ alcohols are produced with a large rate constant via isotope exchange between $CH_{4-n}D_{n-1}OD$ alcohols (the products of C–D bond oxidation) and water molecules.

The KIE calculated from the above product yield ratios and corrected for the number of C–H and C–D bonds in the methane molecule,

$\sigma_n = \{n/(4-n)\}\rho_n = ([CH_{3-n}D_nOH]/[CH_{4-n}D_{n-1}OH])$, increases as the number of deuterium atoms (n) increases and takes the following values:

for CH_3D

$$\begin{aligned} \sigma_1 &= (1/3)\rho_1 \\ &= (1/3)[CH_2DOH]/[CH_3OH] = 3.9 \pm 1.0, \end{aligned}$$

for CH_2D_2

$$\begin{aligned} \sigma_2 &= \rho_2 \\ &= [CHD_2OH]/[CH_2DOH] = 9.30 \pm 0.54, \end{aligned} \quad (2)$$

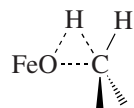
for CHD_3

$$\begin{aligned} \sigma_3 &= 2\rho_3 \\ &= 3[CD_3OH]/[CHD_2OH] = 12.0 \pm 1.0. \end{aligned}$$

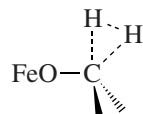
For the oxidation of the $\text{CH}_4 + \text{CD}_4$ mixture under the same conditions [17], the following KIE value was obtained:

$$\sigma_4 = \rho_4 = [\text{CH}_3\text{OH}]/[\text{CD}_3\text{OH}] = 19.3 \pm 3.9. \quad (3)$$

The difference between the KIE values per C–H bond is in conflict with the hidden-radical mechanism, according to which KIE is determined solely by the ratio of the rate constants of C–H and C–D bond homolysis in the methane molecule; i.e., $\sigma_n = [n/(4-n)]\rho_n = k_{\text{H}}/k_{\text{D}}$. At the same time, the simple kinetic scheme of the nonradical mechanism of MMO-catalyzed methane oxidation via the intermediate formation of a pentacoordinated carbon complex, whose first step involves two hydrogen atoms [14], affords an explanation for the unusual distribution of oxidation products of partially deuterated methane (1). Two coexisting forms are suggested for this intermediate complex. One of them, F1, is produced by the addition of an oxygen atom at the C–H bond:



The other form of the intermediate complex, F2, is characterized by a shortened distance between hydrogen atoms:

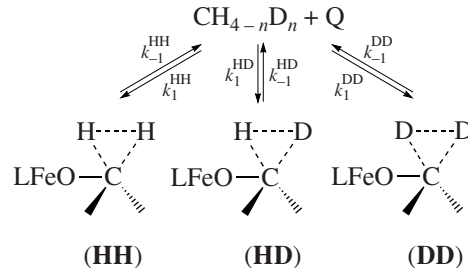


The formation of the intermediate complex is followed by the insertion of an oxygen atom into the C–H bond, which leads to the formation of a hydroxylation product.

The first step in this kinetic scheme is assumed to be the formation of F2. For simplicity, the intermediate complex interconversion reactions will not be considered. An analysis showed [16] that, using parameters with simple physical meanings and plausible values, quantitative agreement between the experimental and calculated hydroxylation product distributions can be achieved only if a fast reaction returning the intermediate complexes into their initial states is introduced. However, it was found [16] that no parameter set simultaneously bringing the calculated data into quantitative agreement with experimental data (1) and (3) exists for this simple mechanism. The region of the parameter space consistent with the observed distribution of hydroxylation products for partially deuterated methane (1) has no overlap with the region of parameters consistent with the KIE value for the oxidation of $\text{CH}_4\text{--CD}_4$ mixture (3).

To eliminate this contradiction, a more complex kinetic model of this mechanism (model I) is analyzed here. In this model, two hydrogen atoms participate simultaneously in the interaction of the intermediate Q (LFeO) with the hydrocarbon; i.e., the first step is the

formation of F2. In the course of methane $\text{CH}_{4-n}\text{D}_n$ oxidation, three types of intermediate species are formed in this first step with the rate constants k_1^{HH} , k_1^{HD} , and k_1^{DD} . These are denoted (HH), (HD), and (DD), according to the composition of their methylene group:



The compounds (HH), (HD), and (DD) are converted back into the initial species $\text{Q} + \text{CH}_{4-n}\text{D}_n$ with the rate constants k_{-1}^{HH} , k_{-1}^{HD} , and k_{-1}^{DD} . In this model, F2 is the main state of the intermediate complex, which determines the statistical coefficients at the rate constants of the reaction steps. Thus, the ratios of intermediate complex production rates w_1 can readily be obtained:

for CH_3D ($n = 1$)

$$w_1^{\text{HH}} : w_1^{\text{HD}} = k_1^{\text{HH}} : k_1^{\text{HD}}, w_1^{\text{DD}} = 0;$$

for CH_2D_2 ($n = 2$)

$$w_1^{\text{HH}} : w_1^{\text{HD}} : w_1^{\text{DD}} = k_1^{\text{HH}} : 4k_1^{\text{HD}} : k_1^{\text{DD}};$$

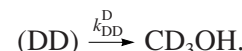
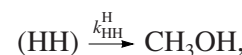
for CHD_3 ($n = 3$)

$$w_1^{\text{HH}} = 0, w_1^{\text{HD}} : w_1^{\text{DD}} = k_1^{\text{HD}} : k_1^{\text{DD}};$$

for CH_4 ($n = 0$) + CD_4 ($n = 4$)

$$w_1^{\text{HD}} = 0, w_1^{\text{HH}} : w_1^{\text{DD}} = k_1^{\text{HH}} : k_1^{\text{DD}}.$$

F1 is implicitly involved in the kinetic scheme and is responsible for the formation of products from F2:



The intermediate compound containing a methylene group with an HD hydrogen bond can yield both a C–H bond oxidation product and a C–D bond oxidation product:



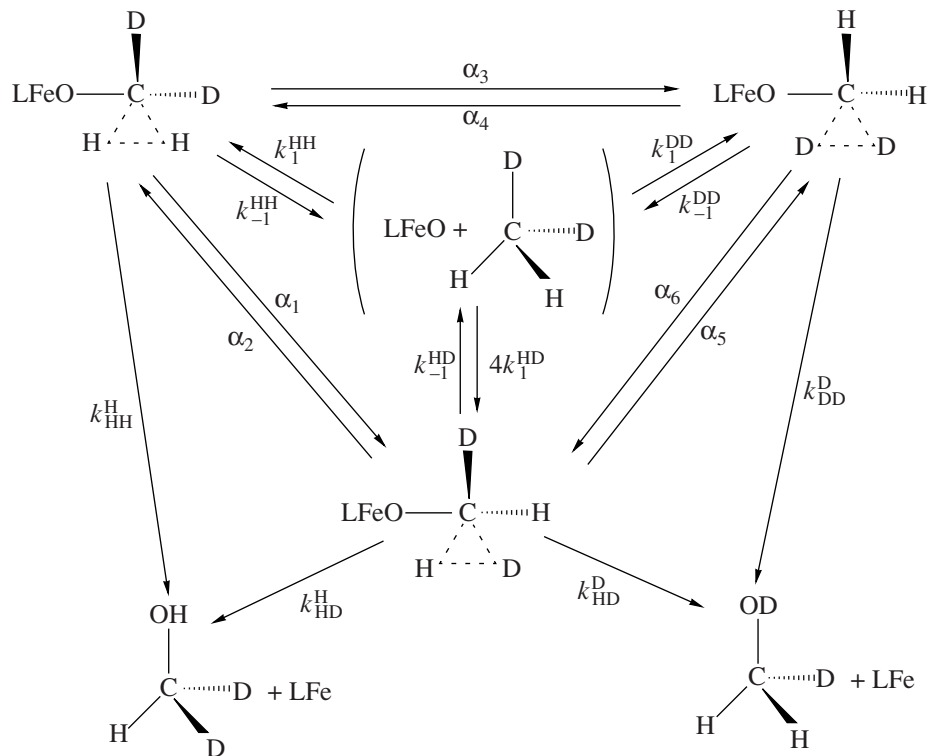
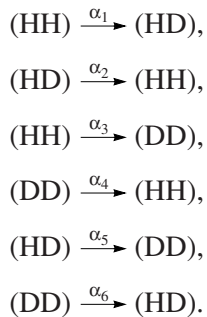


Fig. 2. Kinetic scheme of CH_2D_2 oxidation corresponding to kinetic model I.

The interconversions of F2 species with different methylene groups occur via hydrogen bond replacement:



The F2 isomerization reactions are responsible for the racemization of the reaction products during the MMO-catalyzed oxidation of chiral ethane $\text{H}(3)\text{H}(2)\text{H}(1)\text{CCH}_3$, [8]. These reactions are not included in the kinetic scheme considered here for the reason that chiral methane does not exist.

The CH_2D_2 oxidation kinetic scheme corresponding to this two-step model of the reaction mechanism is shown in Fig. 2. The kinetic schemes of CHD_3 and CH_3D oxidation differ from the CH_2D_2 oxidation scheme only in the values of the numerical coefficients at the rate constants of some steps (Table 1).

Numerical calculations for the CH_2D_2 , CHD_3 , CH_3D , and $\text{CH}_4 + \text{CD}_4$ oxidation kinetic schemes corresponding to this mechanistic model allowed us to find

kinetic parameter ratios ensuring the coincidence of the calculated data both with the experimental product distributions for C–H and C–D bond oxidation in methane (ρ_1 , ρ_2 , and ρ_3 in (1)) and with the KIE value for the oxidation of the CH_4 – CD_4 mixture (ρ_4 in (3)). Rate constant values were set taking into account the steady-state conditions:

$$\ll k_1^{\text{H}\text{H}}, k_1^{\text{H}\text{D}}, k_1^{\text{D}\text{D}}, \alpha_1, \alpha_2, \alpha_3, \alpha_4, \alpha_5, \alpha_6. \quad (4)$$

For example, computations using the kinetic parameter ratios

$$k_1^{\text{HH}} : k_1^{\text{HD}} : k_1^{\text{DD}} = 1 : 1 : 1.$$

$$k_{\perp}^{\text{HH}} : k_{\perp}^{\text{HD}} : k_{\perp}^{\text{DD}} = 1.06 : 1.03 : 1.$$

$$k_{\text{III}}^{\text{H}} : k_{\text{HP}}^{\text{H}} : k_{\text{HP}}^{\text{D}} : k_{\text{DD}}^{\text{D}} \equiv 25.00 : 21.00 : 3.40 : 1.$$

$$\alpha_1 : \alpha_2 : \alpha_3 : \alpha_4 : \alpha_5 : \alpha_6 = 100 : 80 : 65 : 6 : 2 : 1,$$

$$(k_{-1})_{\min}/k_{DD}^D = k_{-1}^{DD}/k_{DD}^D = 10^2,$$

$$(\alpha_i)_{\min}/k_{\text{DD}}^{\text{D}} = \alpha_6/k_{\text{DD}}^{\text{D}} = 10^3$$

under constraint (4) yield $\rho_1 = 12.1$, $\rho_2 = 9.30$, $\rho_3 = 3.90$, and $\rho_4 = 19.3$; for the kinetic parameters ratios

$$k_1^{\text{HH}} : k_1^{\text{HD}} : k_1^{\text{DD}} = 1 : 1 : 1,$$

$$k_{-1}^{\text{HH}} : k_{-1}^{\text{HD}} : k_{-1}^{\text{DD}} = 1.06 : 1.03 : 1,$$

$$k_{\text{HH}}^{\text{H}} : k_{\text{HH}}^{\text{D}} : k_{\text{HD}}^{\text{D}} : k_{\text{DD}}^{\text{D}} = 25.00 : 15.00 : 3.50 : 1,$$

$$\alpha_2 : \alpha_1 : \alpha_4 : \alpha_3 : \alpha_6 : \alpha_5$$

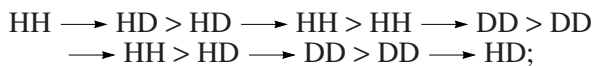
$$= 15.50 : 15.00 : 7.00 : 6.00 : 4.00 : 1,$$

$$(k_{-1})_{\min} / k_{\text{DD}}^{\text{D}} = k_{-1}^{\text{DD}} / k_{\text{DD}}^{\text{D}} = 10^2,$$

$$(\alpha_i)_{\min} / k_{\text{DD}}^{\text{D}} = \alpha_5 / k_{\text{DD}}^{\text{D}} = 10^3,$$

$$\rho_1 = 11.7, \rho_2 = 9.30, \rho_3 = 4.00, \text{ and } \rho_4 = 19.3.$$

Thus, good agreement between the calculated and experimental data can be achieved using realistic values of kinetic parameters. If KIE for hydrogen bond dissociation in the methylene group of F2 is larger than KIE for the formation of this bond, the rate constants α_1 (HH \rightarrow HD) and α_6 (DD \rightarrow HD) will be, respectively, the largest and the smallest in the α_i series. In this case, it is natural to assume the following relationship:



i.e., $\alpha_1 > \alpha_2 > \alpha_3 > \alpha_4 > \alpha_5 > \alpha_6$.

Conversely, if KIE for hydrogen bond dissociation is smaller than KIE for its formation, the smallest rate constant will be α_5 (HD \rightarrow DD), while α_2 (HD \rightarrow HH) can be the largest. The following relationship will then seem natural:

$$\alpha_2 > \alpha_1 > \alpha_4 > \alpha_3 > \alpha_6 > \alpha_5.$$

Note that the above calculations are carried out for the case in which the rate constant of the first reaction step is independent of the isotope composition of the oxidation substrate and the KIE of the reverse reaction is not too large. Under these conditions, the KIE of the second step of methane oxidation must be assigned a sufficiently large value (>20) in order to obtain the experimentally observed value $\rho_4 = 19.3$.

Let us assume that the KIE of the first step of MMO-catalyzed methane hydroxylation has a large value. For example, let us set $k_1^{\text{HH}} : k_1^{\text{HD}} : k_1^{\text{DD}} = 50 : 7 : 1$. In this case, quantitative agreement between the calculated and experimental data can be achieved using the following set of parameter ratios:

$$k_{-1}^{\text{H}} : k_{-1}^{\text{HD}} : k_{-1}^{\text{DD}} = 36.60 : 6.00 : 1,$$

$$(k_{-1})_{\min} / k_{\text{DD}}^{\text{D}} = k_{-1}^{\text{DD}} / k_{\text{DD}}^{\text{D}} = 10,$$

$$(\alpha_i)_{\min} / k_{\text{DD}}^{\text{D}} = \alpha_6 / k_{\text{DD}}^{\text{D}} = 10,$$

$$\alpha_1 : \alpha_2 : \alpha_3 : \alpha_4 : \alpha_5 : \alpha_6 = 120 : 34 : 32 : 30 : 2 : 1,$$

Table 1. Numerical coefficients for the rate constants of the elementary steps of methane isotopomer oxidation according to kinetic model I

Rate constants of elementary steps	CH ₃ D	CH ₂ D ₂	CHD ₃
k_1^{HH}	1	1	0
k_1^{HD}	1	4	1
k_1^{DD}	0	1	1
k_{-1}^{HH}	1	1	0
k_{-1}^{HD}	1	1	1
k_{-1}^{DD}	0	1	1
k_{HH}^{H}	1	1	0
k_{HD}^{H}	1	1	1
k_{HD}^{D}	1	1	1
k_{DD}^{D}	0	1	1
α_1	1	1	0
α_2	1	1	0
α_3	0	1	0
α_4	0	1	0
α_5	0	1	1
α_6	0	1	1

$$k_{\text{HH}}^{\text{H}} : k_{\text{HH}}^{\text{D}} : k_{\text{HD}}^{\text{D}} : k_{\text{DD}}^{\text{D}} = 13.30 : 11.80 : 1.35 : 1$$

$$(\rho_1 = 11.9, \rho_2 = 9.20, \rho_3 = 4.20, \rho_4 = 19.3).$$

For the case $(\alpha_i)_{\min} / k_{\text{DD}}^{\text{D}} = \alpha_5 / k_{\text{DD}}^{\text{D}} = 10$, it is also possible to find parameter ratios that provide quantitative agreement between the calculated and experimental results for the large KIE value of the first step ($k_1^{\text{HH}} : k_1^{\text{HD}} : k_1^{\text{DD}} = 50 : 7 : 1$). Thus, for $\alpha_2 : \alpha_1 : \alpha_4 : \alpha_6 : \alpha_3 : \alpha_5 = 15.00 : 14.00 : 12.00 : 3.00 : 1.20 : 1$ and $k_{\text{HH}}^{\text{H}} : k_{\text{HH}}^{\text{D}} : k_{\text{HD}}^{\text{D}} : k_{\text{DD}}^{\text{D}} = 13.30 : 10.80 : 2.00 : 1$, with all other parameter ratios being the same, one obtains $\rho_1 = 12.6, \rho_2 = 9.20, \rho_3 = 4.00$, and $\rho_4 = 19.3$. Increasing the values of α_i to $(\alpha_i)_{\min} / k_{\text{DD}}^{\text{D}} = \alpha_5 / k_{\text{DD}}^{\text{D}} = 10^2$, one obtains $\rho_1 = 11.9, \rho_2 = 9.30, \rho_3 = 4.00$, and $\rho_4 = 19.3$ at $\alpha_2 : \alpha_1 : \alpha_4 : \alpha_6 : \alpha_3 : \alpha_5 = 10.00 : 9.00 : 6.00 : 5.00 : 2.50 : 1$ and $k_{\text{HH}}^{\text{H}} : k_{\text{HH}}^{\text{D}} : k_{\text{HD}}^{\text{D}} : k_{\text{DD}}^{\text{D}} = 13.30 : 8.80 : 2.00 : 1$ without changing the other parameters. Comparison of the above parameter ratios shows that increasing the $(\alpha_i)_{\min} / (k_{-1})_{\min}$ ratio allows one to diminish the difference between the largest and the smallest α_i values.

Table 2. Numerical coefficients for the rate constants of the interconversions of the intermediate complexes F2 containing pentacoordinated carbon according to kinetic model II

Interconversion rate constants	CH ₃ D	CH ₂ D ₂	CHD ₃
α_1	3	4	0
α_2	3	1	0
α_3	0	1	0
α_4	0	1	0
α_5	0	1	3
α_6	0	1	3
α_7	3	1	0
α_8	3	4	3
α_9	0	1	3

Special consideration should be given to the parameter $h = k_{-1}^{\text{DD}}/k_{\text{DD}}^{\text{D}}$, which defines the reaction rate ratio for the conversion of the intermediate complexes into alcohols and the initial reagents. In the case of $h = 1$, the following parameter sets reproduce the experimental product distribution and the KIE of methane oxidation:

$$(k_{-1})_{\min}/k_{\text{DD}}^{\text{D}} = k_{-1}^{\text{DD}}/k_{\text{DD}}^{\text{D}} = 1,$$

$$k_1^{\text{HH}} : k_1^{\text{HD}} : k_1^{\text{DD}} = 50.00 : 7.00 : 1,$$

$$k_{-1}^{\text{HH}} : k_{-1}^{\text{HD}} : k_{-1}^{\text{DD}} = 55.60 : 7.35 : 1,$$

$$k_{\text{HH}}^{\text{H}} : k_{\text{HD}}^{\text{H}} : k_{\text{DD}}^{\text{H}} : k_{\text{DD}}^{\text{D}} = 13.30 : 11.50 : 1.28 : 1,$$

$$(\alpha_i)_{\min}/k_{\text{DD}}^{\text{D}} = \alpha_6/k_{\text{DD}}^{\text{D}} = 1,$$

$$\alpha_1 : \alpha_2 : \alpha_3 : \alpha_4 : \alpha_5 : \alpha_6 = 200 : 40 : 32 : 30 : 2 : 1$$

$$(\rho_1 = 11.9, \rho_2 = 9.30, \rho_3 = 3.90, \rho_4 = 19.3);$$

or (the other parameter ratios are the same as above)

$$(\alpha_i)_{\min}/k_{\text{DD}}^{\text{D}} = \alpha_5/k_{\text{DD}}^{\text{D}} = 1,$$

$$\alpha_2 : \alpha_1 : \alpha_4 : \alpha_6 : \alpha_3 : \alpha_5 = 100 : 90 : 60 : 30 : 20 : 1,$$

$$k_{\text{HH}}^{\text{H}} : k_{\text{HD}}^{\text{H}} : k_{\text{DD}}^{\text{H}} : k_{\text{DD}}^{\text{D}} = 13.30 : 9.00 : 2.10 : 1$$

$$(\rho_1 = 12.6, \rho_2 = 9.20, \rho_3 = 4.10, \rho_4 = 19.3).$$

Changing the $(\alpha_i)_{\min}/(k_{-1})_{\min}$ ratio again makes it possible to vary the difference between the largest and the smallest α_i values. For instance, at the invariable parameter ratios

$$(k_{-1})_{\min}/k_{\text{DD}}^{\text{D}} = k_{-1}^{\text{DD}}/k_{\text{DD}}^{\text{D}} = 1,$$

$$k_1^{\text{HH}} : k_1^{\text{HD}} : k_1^{\text{DD}} = 50.00 : 7.00 : 1,$$

$$k_{-1}^{\text{HH}} : k_{-1}^{\text{HD}} : k_{-1}^{\text{DD}} = 55.60 : 7.35 : 1,$$

agreement between the calculated and experimental product distributions and KIE values for methane oxidation is achieved in the following cases:

for $(\alpha_i)_{\min}/k_{\text{DD}}^{\text{D}} = \alpha_6/k_{\text{DD}}^{\text{D}} = 1$, with the parameter ratios

$$\alpha_1 : \alpha_2 : \alpha_3 : \alpha_4 : \alpha_5 : \alpha_6 = 180 : 40 : 32 : 30 : 1.5 : 1,$$

$$k_{\text{HH}}^{\text{H}} : k_{\text{HD}}^{\text{H}} : k_{\text{DD}}^{\text{H}} : k_{\text{DD}}^{\text{D}} = 13.30 : 11.50 : 1.31 : 1$$

$$(\rho_1 = 11.9, \rho_2 = 9.20, \rho_3 = 4.10, \rho_4 = 19.3);$$

for $(\alpha_i)_{\min}/k_{\text{DD}}^{\text{D}} = \alpha_6/k_{\text{DD}}^{\text{D}} = 0.1$, with the parameter ratios

$$\alpha_1 : \alpha_2 : \alpha_3 : \alpha_4 : \alpha_5 : \alpha_6 = 500 : 50 : 32 : 30 : 2 : 1,$$

$$k_{\text{HH}}^{\text{H}} : k_{\text{HD}}^{\text{H}} : k_{\text{DD}}^{\text{H}} : k_{\text{DD}}^{\text{D}} = 13.30 : 11.00 : 1.25 : 1$$

$$(\rho_1 = 12.8, \rho_2 = 9.30, \rho_3 = 4.10, \rho_4 = 19.3);$$

for $(\alpha_i)_{\min}/k_{\text{DD}}^{\text{D}} = \alpha_6/k_{\text{DD}}^{\text{D}} = 10$, with the parameter ratios

$$\alpha_1 : \alpha_2 : \alpha_3 : \alpha_4 : \alpha_5 : \alpha_6 = 111 : 37 : 32 : 30 : 1.5 : 1,$$

$$k_{\text{HH}}^{\text{H}} : k_{\text{HD}}^{\text{H}} : k_{\text{DD}}^{\text{H}} : k_{\text{DD}}^{\text{D}} = 13.30 : 11.50 : 1.35 : 1$$

$$(\rho_1 = 11.9, \rho_2 = 9.20, \rho_3 = 4.00, \rho_4 = 19.3).$$

For $h = 10^3$, it is also possible to find parameter sets reproducing the specified product distribution and KIE of methane oxidation. For example,

$$(k_{-1})_{\min}/k_{\text{DD}}^{\text{D}} = k_{-1}^{\text{DD}}/k_{\text{DD}}^{\text{D}} = 10^3,$$

$$(\alpha_i)_{\min}/k_{\text{DD}}^{\text{D}} = \alpha_5/k_{\text{DD}}^{\text{D}} = 10^4,$$

$$k_1^{\text{HH}} : k_1^{\text{HD}} : k_1^{\text{DD}} = 50.00 : 7.00 : 1,$$

$$k_{-1}^{\text{HH}} : k_{-1}^{\text{HD}} : k_{-1}^{\text{DD}} = 34.50 : 5.80 : 1,$$

$$k_{\text{HH}}^{\text{H}} : k_{\text{HD}}^{\text{H}} : k_{\text{DD}}^{\text{H}} : k_{\text{DD}}^{\text{D}} = 13.30 : 10.00 : 2.10 : 1,$$

$$\alpha_2 : \alpha_1 : \alpha_4 : \alpha_6 : \alpha_3 : \alpha_5 = 15 : 15 : 6 : 3 : 2 : 1$$

$$(\rho_1 = 11.1, \rho_2 = 9.30, \rho_3 = 4.10, \rho_4 = 19.3).$$

Note that, in all cases, the ratios of α_i are minimized if $(\alpha_i)_{\min} \gg (k_{-1})_{\min}$.

Calculations of the kinetic schemes of methane isotopomer oxidation, whose results are presented above, do not take into account the statistical coefficients at the rate constants of the interconversions of the intermediate complexes F2 with different methylene groups (HH, HD, and DD). It should be noted that different mechanisms and, correspondingly, different coefficient values are possible for these interconversion reactions. By setting these coefficients in accordance with the selected mechanism, appropriate kinetic parameter ratios can easily be found. Table 2 shows statistical coefficients for the rate constants α_i for one of the possible mechanisms (kinetic model II), in which the dissociation of the hydrogen bonds in the methylene groups does not

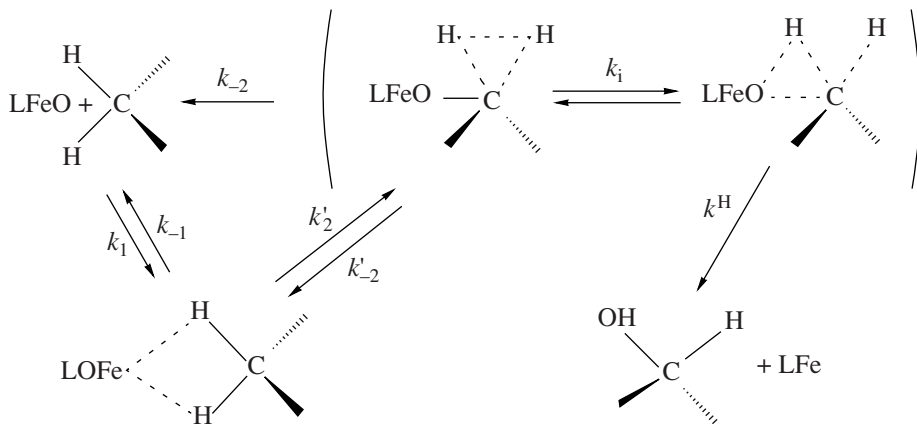


Fig. 3. Multistep nonradical mechanism of the monooxygenase-catalyzed oxidation of alkanes.

involve free hydrogen atoms and is followed by the formation of new F2 species according to the isotope composition of the oxidation substrate. In this case, statistics requires that the possibility of the formation of a hydrogen bond with the same isotope composition after its dissociation should be taken into account. To do this, the rate constants α_7 ($\text{HH} \rightarrow \text{HH}$), α_8 ($\text{HD} \rightarrow \text{HD}$), and α_9 ($\text{DD} \rightarrow \text{DD}$) are introduced. Numerical calculations for the CH_2D_2 , CHD_3 , CH_3D , and $\text{CH}_4 + \text{CD}_4$ oxidation kinetic schemes corresponding to this choice of reaction mechanism allow one to find parameter ratios ensuring agreement between the calculated and experimental product distribution and KIE data. For example, under the quasi-steady-state conditions

$$k_1^{\text{HH}}, k_1^{\text{HD}}, k_1^{\text{DD}} \quad (5)$$

$$\ll k_{\text{HH}}^{\text{H}}, k_{\text{HD}}^{\text{H}}, k_{\text{DD}}^{\text{D}}, \alpha_1, \alpha_2, \alpha_3, \alpha_4, \alpha_5, \alpha_6, \alpha_7, \alpha_8, \alpha_9$$

for the parameter ratios

$$k_1^{\text{HH}} : k_1^{\text{HD}} : k_1^{\text{DD}} = 50.00 : 7.00 : 1,$$

$$k_{-1}^{\text{HH}} : k_{-1}^{\text{HD}} : k_{-1}^{\text{DD}} = 55.60 : 7.35 : 1,$$

$$k_{\text{HH}}^{\text{H}} : k_{\text{HD}}^{\text{H}} : k_{\text{DD}}^{\text{D}} : k_{\text{DD}}^{\text{D}} = 13.30 : 11.40 : 1.17 : 1,$$

$$\alpha_7 : \alpha_1 : \alpha_2 : \alpha_3 : \alpha_8 : \alpha_4 : \alpha_5 : \alpha_6 : \alpha_9 = 400 : 270 : 40.00 : 32.00 : 30.00 : 30.00 : 2.40 : 1.35 : 1,$$

$$(k_{-1})_{\min} / k_{\text{DD}}^{\text{D}} = k_{-1}^{\text{DD}} / k_{\text{DD}}^{\text{D}} = 1,$$

$$(\alpha_i)_{\min} / k_{\text{DD}}^{\text{D}} = \alpha_5 / k_{\text{DD}}^{\text{D}} = 1,$$

one obtains

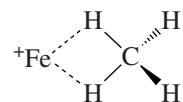
$$\rho_1 = 11.7, \rho_2 = 9.30, \rho_3 = 4.00, \rho_4 = 19.3.$$

Likewise, one can easily find kinetic parameter sets corresponding to the other F2 interconversion variants.

Thus, the kinetic schemes of methane oxidation corresponding to the mechanism involving the reversible formation of the FeO---CH_4 complex were analyzed

using numerical methods. In the case where there is one C—H and one C—D bond at the carbon atom being oxidized (the other two bonds are with C atoms), the kinetic schemes considered here can be reduced to the simple kinetic scheme suggested earlier, which is in excellent agreement with the experimental data available on the hydroxylation of hydrocarbons with this structure by cytochrome P450 [11]. Thus, experimental data on the monooxygenase oxidation of alkanes by different enzyme systems can be explained in the framework of the same nonradical mechanism.

In a more recent study [18], a different modification of the two-step nonradical mechanism was put forth based on numerical computations using density functional theory (DFT). This mechanism postulates the formation of an intermediate complex between methane and an active site of MMO via the interaction of carbon and iron atoms: OFe---CH_4 . These calculations demonstrated that the formation of the intermediate complex $\text{Fe}^+---\text{CH}_4$ both in the low-spin and high-spin states involves two hydrogen atoms, yielding $\eta^2\text{-H}_2\text{H}$ -type bonds [18]:



The second step of this mechanism is the migration of a hydrogen atom and a methyl group, which yields a product containing methanol as a ligand. The coordination of the alkane to an electrophilic site in the first step should lead to the weakening of the C—H bonds—a feature making this mechanism very attractive. However, this mechanism provides no explanation for the isomerization of partially deuterated alkanes in the course of enzymatic oxidation by cytochrome P450.

As we pointed out earlier [14], the nonradical mechanism of alkane oxidation by monooxygenases is quite complicated and is possibly a superposition of two nonradical mechanisms. The following kinetic scheme can be suggested as a possible variant of this mechanism. In

the first step, the alkane molecule interacts with the iron-containing electrophilic site (Fig. 3). The second step is the formation of an intermediate complex containing a pentacoordinated carbon atom. The assumption about the formation of this complex is supported by the partial racemization of enzymatic oxidation products observed experimentally for chiral molecules of monodeuteroethylbenzene PhCHDCH_3 [19] and ethane H(3)H(2)H(1)CCH_3 [8]. Furthermore, the hypothesis about the formation of such an intermediate complex is in quantitative agreement with experimental product distribution data for the hydroxylation of deuterated camphor stereoisomers in a natural system [20]. As we pointed out above, these data cannot be explained in the framework of the radical oxygen rebound mechanism, which is widely accepted for alkane oxidation by monooxygenases.

In the light of the above arguments, let us analyze model III of the nonradical multistep mechanism of MMO-catalyzed methane oxidation. Let us assume that the first step of the interaction between the intermediate Q (LFeO) and the $\text{CH}_{4-n}\text{D}_n$ molecule, which involves two hydrogen atoms, reversibly yields the complex LFeO--CH_{4-n}D_n (with the forward rate constants k_1^{HH} , k_1^{HD} , k_1^{DD} and the reverse rate constants k_{-1}^{HH} , k_{-1}^{HD} , and k_{-1}^{DD} , respectively). The next step, in which the complex LFeO--CH_{4-n}D_n is formed, also involves two hydrogen atoms; i.e., the complexes F2 appear with rate constants k_2^{HH} , k_2^{HD} , and k_2^{DD} . It is assumed that the rate constant of the reverse reaction LFeO--CH_{4-n}D_n \rightarrow LFeO--CH_{4-n}D_n (k_{-2}') is negligible compared to the decomposition rate constant of the intermediate complex containing pentacoordinated carbon. In this case, the complex LFeO--CH_{4-n}D_n can either return into the initial state (Q + CH_{4-n}D_n) with the rate constant k_{-2} (k_{-2}^{HH} , k_{-2}^{HD} , and k_{-2}^{DD} , depending on the isotope composition) or form the oxidation product CH_{3-n}D_nOH with the corresponding rate constant (k_{HH}^{H} , k_{HD}^{H} , k_{HD}^{D} , k_{DD}^{D}). As in model I for the two-step mechanism analyzed above, we assume that the F2 complexes with different isotope compositions of methylene groups can be converted into each other with the rate constants α_1 , α_2 , α_3 , α_4 , α_5 , and α_6 .

The kinetic scheme of CH₂D₂ oxidation corresponding to model III of the multistep mechanism is shown in Fig. 4. The kinetic schemes of CHD₃ and CH₃D oxidation differ from the CH₂D₂ oxidation scheme only in numerical coefficients at the rate constants of certain reaction steps.

Numerical calculations for the CH₂D₂, CHD₃, CH₃D, and CH₄ + CD₄ oxidation kinetic schemes corresponding to this kinetic model (for the latter case, the

kinetic scheme is shown in Fig. 5) under the quasi-steady-state conditions

$$\begin{aligned} k_1^{\text{HH}}, k_1^{\text{HD}}, k_1^{\text{DD}} &\ll k_2^{\text{HH}}, k_2^{\text{HD}}, k_2^{\text{DD}} \\ &\ll k_{\text{HH}}^{\text{H}}, k_{\text{HD}}^{\text{H}}, k_{\text{HD}}^{\text{D}}, k_{\text{DD}}^{\text{D}}, \alpha_1, \alpha_2, \alpha_3, \alpha_4, \alpha_5, \alpha_6, \end{aligned} \quad (6)$$

allowed us to find a set of kinetic parameter ratios providing good agreement between calculated and experimental data on product distribution in the oxidation of C–H and C–D bonds and on the KIE of CH₄–CD₄ mixture oxidation. For example, ignoring the specific mechanism of F2 interconversions, one obtains $\rho_1 = 11.9$, $\rho_2 = 9.30$, $\rho_3 = 4.00$, and $\rho_4 = 19.3$ using the following kinetic parameter ratios:

$$k_1^{\text{HH}} : k_1^{\text{HD}} : k_1^{\text{DD}} = 50.00 : 7.00 : 1,$$

$$k_{-1}^{\text{HH}} : k_{-1}^{\text{HD}} : k_{-1}^{\text{DD}} = 4.00 : 2.00 : 1,$$

$$k_2^{\text{HH}} : k_2^{\text{HD}} : k_2^{\text{DD}} = 1 : 1 : 1,$$

$$k_{-2}^{\text{HH}} : k_{-2}^{\text{HD}} : k_{-2}^{\text{DD}} = 2.10 : 1.45 : 1,$$

$$k_{\text{HH}}^{\text{H}} : k_{\text{HD}}^{\text{H}} : k_{\text{HD}}^{\text{D}} : k_{\text{DD}}^{\text{D}} = 7.00 : 6.00 : 1.25 : 1,$$

$$\alpha_2 : \alpha_1 : \alpha_4 : \alpha_6 : \alpha_3 : \alpha_5 = 11.00 : 9.00 : 7.00 : 5.00 : 2.00 : 1,$$

$$(k_{-1})_{\text{min}} / k_{\text{DD}}^{\text{D}} = k_{-1}^{\text{DD}} / k_{\text{DD}}^{\text{D}} = 1,$$

$$(k_{-2})_{\text{min}} / k_{\text{DD}}^{\text{D}} = k_{-2}^{\text{DD}} / k_{\text{DD}}^{\text{D}} = 1,$$

$$(\alpha_i)_{\text{min}} / k_{\text{DD}}^{\text{D}} = \alpha_5 / k_{\text{DD}}^{\text{D}} = 10.$$

In this case, as in the two-step mechanism, the largest KIE value was chosen for the first reaction step for the reason that the kinetic scheme suggested is just one of the possible variants of the nonradical mechanism, which can actually involve a larger number of steps. Depending on the particular mechanism considered, the largest KIE value may be assigned to a reaction step other than the first.

The above results of numerical calculations demonstrate that the kinetic schemes support many sets of kinetic parameters ensuring good agreement between the calculated data and experimental data (2) and (3) provided that the interconversion rate of the F2 complexes with different methylene groups is sufficiently high.

Once again, it should be emphasized that the three-step scheme considered here is only one of the many possible variants of the nonradical mechanism of alkane oxidation by monooxygenases. The main result of this study is the explanation of many experimental results obtained in various studies in the framework of a unified mechanism based on the hypothesis of synchronous insertion of an oxygen atom into the C–H bond, with an important new feature: an intermediate complex between active oxygen and the hydrocarbon molecule is formed prior to insertion. The crucial role

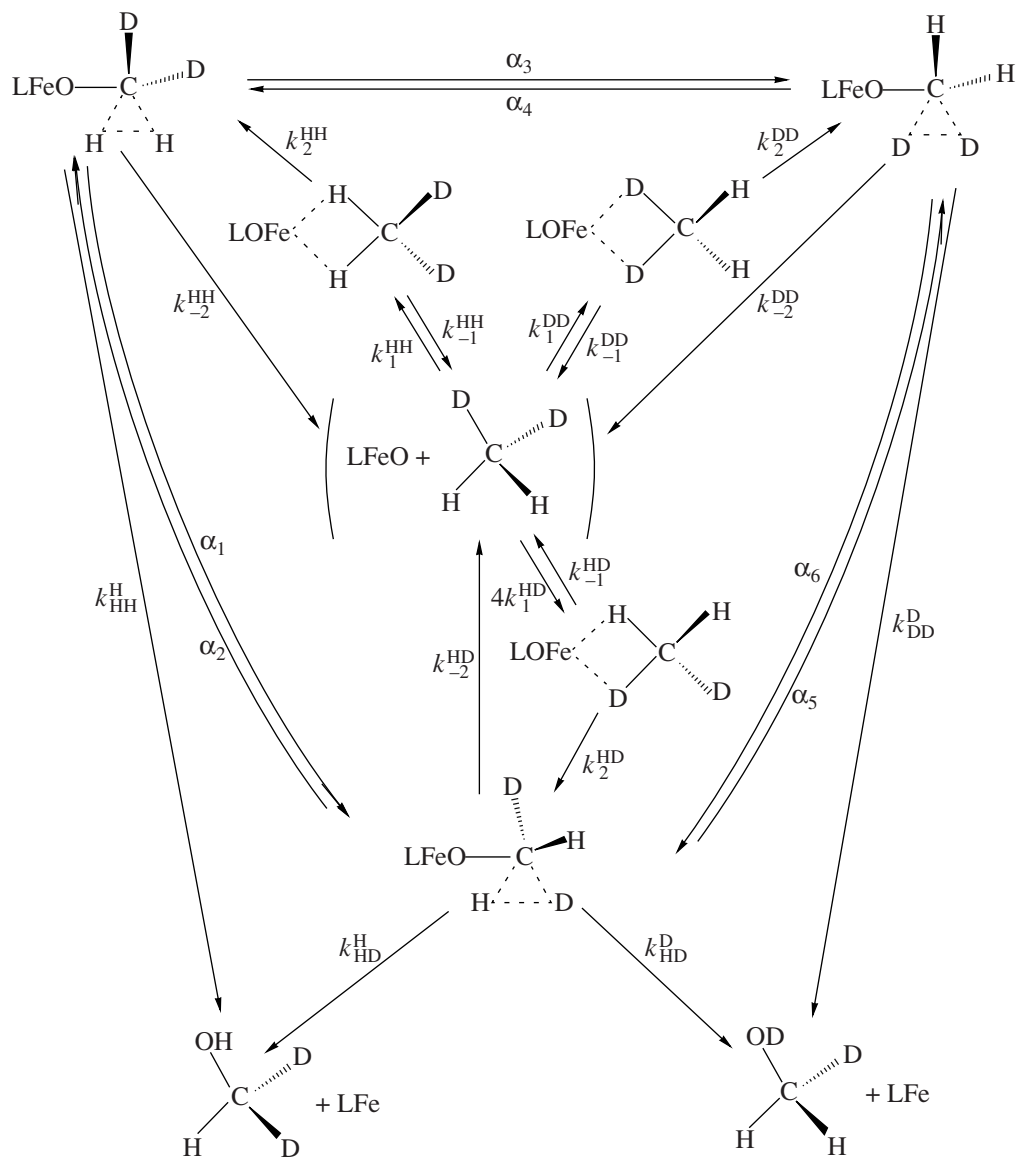


Fig. 4. Kinetic scheme of CH_2D_2 oxidation corresponding to kinetic model III.

in the formation of this complex is played by the oxygen atom, while the metal atom serves as its ligand. The substrate structure in this complex with active oxygen is highly distorted and contains pentacoordinated carbon. Two hydrogen atoms (or a hydrogen atom and a deuterium atom) in this complex can relatively easily exchange their places, which leads to the racemization of the oxidation products. The particular mechanism of the formation of this complex will be investigated in future work by quantum mechanical means. For this reason, the main focus of the present study was on a simpler, two-step mechanism. The numerical calculations for the above three-step mechanism only indicate that it is possible to complicate the nonradical mechanism without giving rise to new contradictions with experimental data.

An earlier analysis [16] showed that quantitative agreement between experimental and calculated product distribution data for the MMO-catalyzed hydroxylation of partially deuterated methane (CH_3D , CH_2D_2 , CHD_3) can be achieved using kinetic parameters with simple physical meanings and realistic values only if the reverse reaction converting the intermediate complexes into the initial reactants is introduced. Note the following important feature of methane oxidation catalyzed by MMO: the decomposition rate of the intermediate complex containing pentacoordinated carbon is significantly higher than the rate of its formation. If this complex is formed in several steps, its decomposition into the initial reactants may either proceed via the complete reverse sequence of these steps or bypass the formation of some intermediates, possibly consisting of

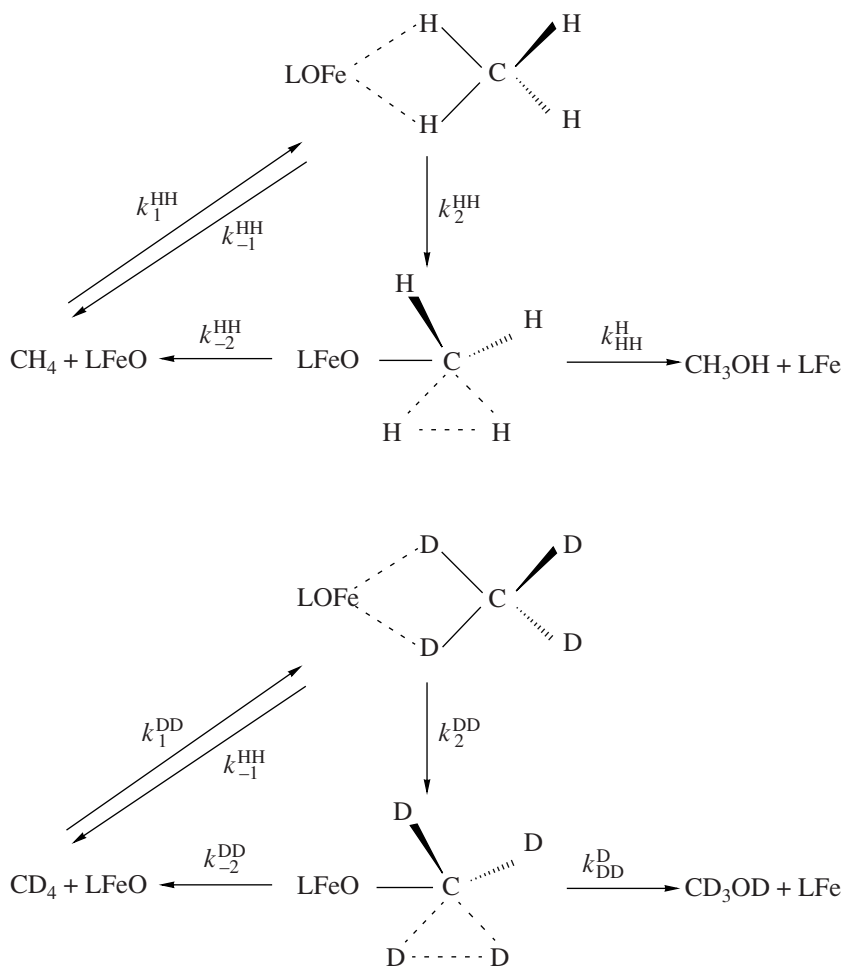


Fig. 5. Kinetic scheme of CH_4 – CD_4 mixture oxidation corresponding to kinetic model III.

a single step. The particular variant of this mechanism will be determined by the detailed balancing principle, specifically, the densities of states, their energy differences, and whether or not the transitions between certain states are spin-forbidden. The experimental data on the oxidation of chiral ethane $\text{H}(3)\text{H}(2)\text{H}(1)\text{CCH}_3$ by MMO [8] are in quantitative agreement with the nonradical mechanism suggested here, regardless of whether the formation of the intermediate complex with pentacoordinated carbon is irreversible [15] or not.

Thus, the unusual experimental data obtained in earlier studies on the oxidation of different alkanes by the MMO enzyme system are explained for the first time in the framework of a unified multistep nonradical mechanism. Further investigation of alkane monooxygenation dynamics requires quantum mechanical calculations taking into account the results of this study.

REFERENCES

1. Groves, J.T., *J. Inorg. Biochem.*, 2006, vol. 100, no. 4, p. 434.
2. Lieberman, R.L. and Rosenzweig A.C., *Nature*, 2005, vol. 434, no. 10, p. 177.
3. Poulos, T.L., *Biochem. Biophys. Res. Commun.*, 2005, vol. 338, no. 1, p. 337.
4. Lipscomb, J.D., *Annu. Rev. Microbiol.*, 1994, no. 48, p. 371.
5. Feig, A.L. and Lippard, S.J., *Chem. Rev.*, 1994, vol. 94, p. 759.
6. Nesheim, J.C. and Lipscomb, J.D., *J. Inorg. Biochem.*, 1995, vol. 59, no. 1, p. 369.
7. Valentine, A.M., Stahl, S.S., and Lippard, S.J., *J. Am. Chem. Soc.*, 1999, vol. 121, no. 16, p. 3876.
8. Priestley, N.D., Floss, H.G., Froland, W.A., Lipscomb, J.D., Williams, P.G., Morimoto, H., *J. Am. Chem. Soc.*, 1992, vol. 114, no. 19, p. 7561.
9. Friesner, R.A., Baik, M.-H., Gherman, B.F., Guallar, V., Wirstam, M., Murphy, R.B., Lippard, S.J., *Coord. Chem. Rev.*, 2003, nos. 238–239, p. 267.
10. Groves, J.T., *J. Chem. Educ.*, 1985, vol. 62, no. 1, p. 928.
11. Karasevich, E.I., Shestakov, A.F., and Shilov, A.E., *Kinet. Katal.*, 1997, vol. 38, no. 6, p. 852 [*Kinet. Catal. (Engl. Transl.)*, vol. 38, no. 6, p. 782].

12. Karasevich, E.I., Kulikova, V.S., Shilov, A.E., and Shtainman, A.A., *Usp. Khim.*, 1998, vol. 67, no. 4, p. 376 [*Russ. Chem. Rev.*, vol. 67, no. 4, p. 335].
13. Shestakov, A.F. and Shilov, A.E., *J. Mol. Catal.*, 1996, vol. 105, no. 1, p. 1.
14. Karasevich, E.I., Karasevich, Yu.K., Shestakov, A.F., and Shilov, A.E., *Kinet. Katal.*, 2003, vol. 44, no. 1, p. 122 [*Kinet. Catal. (Engl. Transl.)*, vol. 44, no. 1, p. 112].
15. Karasevich, E.I., Karasevich, Yu.K., Shestakov, A.F., and Shilov, A.E., *Kinet. Katal.*, 2003, vol. 44, no. 2, p. 266 [*Kinet. Catal. (Engl. Transl.)*, vol. 44, no. 2, p. 247].
16. Karasevich, E.I., *Kinet. Katal.*, 2007, vol. 48, no. 3 [*Kinet. Catal. (Engl. Transl.)*, vol. 48, no. 3] (in press).
17. Nesheim, J.C. and Lipscomb, J.D., *Biochemistry*, 1996, vol. 35, no. 31, p. 10240.
18. Yoshizawa, K., *J. Organomet. Chem.*, 2001, vol. 635, no. 1, p. 100.
19. White, R.E., Miller, J.P., Favreau, L.V., et al., *J. Am. Chem. Soc.*, 1986, vol. 104, no. 19, p. 6024.
20. Gelb, M.H., Heimbrook, D.C., Malkonen, P., et al., *Biochemistry*, 1982, vol. 21, no. 2, p. 370.